ELSEVIER

Surface Science 409 (1998) 199–206

surface science

Interaction of O_2 with WC(0001)

J. Brillo, H. Kuhlenbeck *, H.-J. Freund

Fritz-Haber-Institut der Max-Planck-Gesellschaft, Abteilung Chemische Physik, Faradayweg 4–6, D-14195 Berlin, Germany

Received 3 September 1997; accepted for publication 24 February 1998

Abstract

We report ARUPS, TDS and AUGER data for the interaction of O_2 with WC(0001). Depending on the preparation conditions, the adsorption of O_2 leads to different compounds on the surface. Exposure to several millibars of O_2 induces the formation of WO_3 with no carbon left on the surface. The tungsten trioxide may be reduced towards WO_2 by annealing in an H_2 atmosphere. Less intensive oxygen treatment (some 10^{-5} mbar) leads, depending on the oxygen pressure and surface temperature, to elemental tungsten, tungsten oxide and carboxide in the surface region with the elemental tungsten being covered by a thin oxide layer. At elevated temperatures, oxygen reacts with the carbon and desorbs as CO, as observed via TDS and ARUPS.

Keywords: Angle-resolved photoemission; Auger electron spectroscopy; Oxygen; Thermal desorption spectroscopy; Tungsten carbide

1. Introduction

Early transition metal carbides display interesting physical and chemical properties. Their melting points are above 3300 K and their hardness is very high [1]. Electronic and magnetic properties such as electrical and thermal conductivity, Hall-coefficient, magnetic susceptibility and heat capacity are metal-like [2]. They also finally exhibit a catalytic activity that is similar to that of some noble metals like Pt, Pd, Rh and Ru [3–6]. Tungsten carbide, for instance, is used as a catalyst for the recombination reaction of hydrogen and oxygen in batteries [7,8]. An overview of available data for transition metal carbides, including thin films and powder samples, is given in [9–11].

WC reacts strongly with NO and CO and dissociates these molecules at temperatures, even below 300 K [12]. It has also been shown to be active for hydrogenation and dehydrogenation reactions and it decomposes hydrocarbons [13,14]. The reactivity is strongly dependent on the surface composition [14–16]. There is still an open discussion in literature as to whether the activity of tungsten carbide is related to regular carbide, carbon and/or oxygen impurities or even to tungsten oxide. However, most studies point towards an involvement of oxygen [14–17].

Until now, there have not been many studies reported on single crystalline tungsten carbide, which may be due to the limited availability of single crystals. The electronic structure has been probed using photoemission by Johansson et al. [18] and some adsorption data (CO, O_2) are reported in [19,20]. Håkanson and Johansson [19] presented the first results on the interaction of oxygen with a single crystalline WC(0001) surface.

* Corresponding author. Fax: (+49) 30 84134307; e-mail: kuhlenbeck@fhi-berlin.mpg.de

0039-6028/98/$19.00
PII: S0039-6028(98)00193-9

They report the formation of WO and chemisorbed oxygen, but no oxycarbides could be identified.

The aim of this work is to develop a detailed picture of the WC(0001)–O_2 interaction as a function of preparation temperature and oxygen pressure. For our investigations, we employed angular-resolved photoemission (ARUPS) of the valence band and the W4f levels, Auger electron spectroscopy (AES) and thermal desorption spectroscopy (TDS).

2. Experimental

The experiments were performed in an UHV system that is equipped with facilities for sample preparation, angular-resolved photoemission spectroscopy (ARUPS), Auger electron spectroscopy (AES) and thermal desorption spectroscopy (TDS), using a differentially pumped quadrupole mass spectrometer equipped with a so-called Feulner cup [21]. For the ARUPS experiments, light from the TGM3 monochromator at the BESSY synchrotron radiation center in Berlin was used.

The sample was attached to two tantalum wires (0.25 mm in thickness) that were spot-welded to two tungsten rods (1 mm in thickness). These were plugged into a sapphire block connected to a liquid nitrogen reservoir so that the sample could be cooled down to $T \approx 90$ K. Heating was possible either by electron impact or by heat radiation from a filament mounted behind the backside of the crystal. With this setup, temperatures of more than 2000 K could be reached. The sample temperature was determined with a W–Re 26%/W–Re 95% thermocouple spot-welded to one of the tantalum wires at a point where the latter was in direct contact with the crystal.

The WC(0001) sample has been cut off from a tungsten carbide block after orientation with Laue backscattering. It contained a large amount of iron that was removed prior to polishing by annealing at $T \geq 2000$ K in UHV. Thereafter, the sample was polished using standard procedures. The main impurity found during preparation was sulfur, which segregated out of the bulk. This was removed by heating at $T \geq 1300$ K and/or sputtering. The W/C stoichiometry of the sample was adjusted by annealing in an oxygen atmosphere at $T \geq 1300$ K in the case of excess carbon on the surface or by glowing in an atmosphere of about 10^{-4} mbar of CH_4 if the surface was carbon-deficient.

The stoichiometry and chemical state of the carbon in the surface regime were checked with AES. Carbidic carbon is characterized by an AES spectrum with two well-defined satellites at kinetic energies somewhat less than that of the main peak. These are missing for graphitic carbon (see Fig. 1). Prolonged annealing at $T \approx 1600$ K turned out to be a suitable method for transforming graphitic carbon into its carbidic form.

3. Results and discussion

The interaction of the WC(0001) surface with oxygen was studied using ARUPS, AES and TDS. A TDS spectrum ($m/e = 28$) is shown in Fig. 2. In this spectrum, two strong CO desorption peaks at $T \approx 750$ K and $T \approx 890$ K are observed, clearly showing that the interaction with oxygen leads to removal of carbon atoms at a higher temperature.

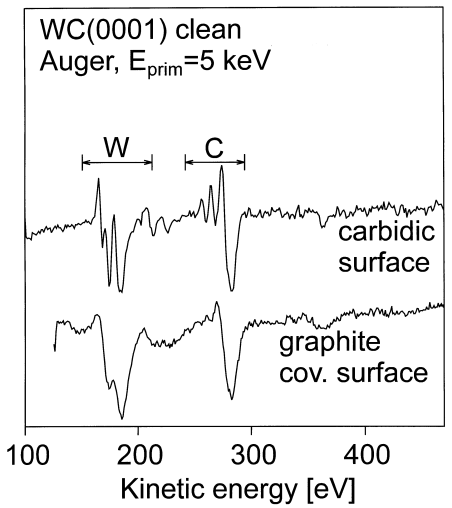

Fig. 1. Auger spectra of WC(0001) with carbidic and graphitic carbon on the surface. The graphite-covered surface was prepared by annealing the sample at $T \approx 1300$ K in an atmosphere of 10^{-4} mbar of CH_4, whereas the carbidic surface was obtained after prolonged annealing at $T \approx 1600$ K in a vacuum.

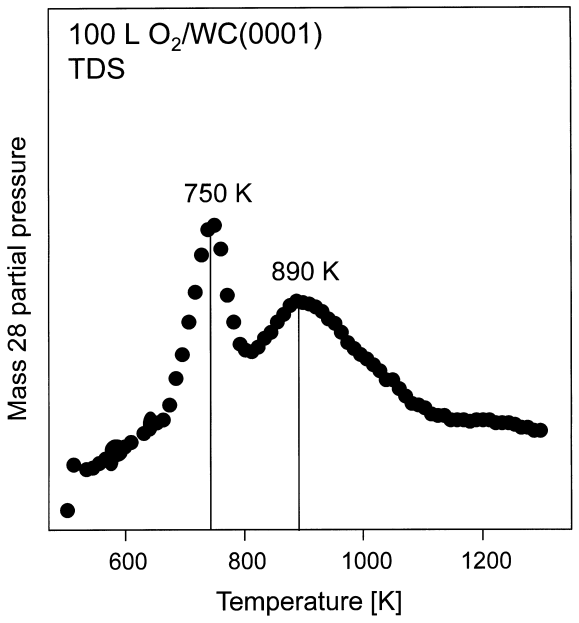

Fig. 2. Thermal desorption spectrum of 100 L of oxygen on WC(0001). Oxygen was admitted at a pressure of 10^{-7} mbar while the surface was at a temperature of $T \approx 80$ K. The mass spectrometer was set to $m/e = 28$ during the scan.

A possible desorption mechanism might be that at 750 K, the surface carbon is reacted away, leading to the first desorption state, and at 890 K, the remaining oxygen reacts with carbon in the second and higher layers. As will be discussed below, oxygen is able to remove carbon from deeper layers, thus supporting this explanation.

A set of electron spectroscopic data of O_2 on WC(0001) is depicted in Fig. 3. The $W4f_{7/2}$ spectrum of the clean surface (Fig. 3a, bottom) consists of two peaks that we assign to a bulk (31.6 eV) and a surface state (31.3 eV) in agreement with the literature data [22,23].

After dosing of 2000 L of O_2 at $T \approx 80$ K, the intensity of the surface state decreases strongly, but surprisingly, it recovers at higher dosing temperatures. The attenuation of this feature at 31.3 eV upon oxygen dosing is a strong indication that it is a surface state of the clean WC(0001) surface quenched by the presence of an adsorbate. However, the peak appearing on the oxygen dosed surfaces at a higher temperature must have a different origin.

Oxygen dosing at 1300 K (spectra at the top in Fig. 3) leads to a loss of all carbon in the surface region as judged from the corresponding AES spectrum. This is in line with the TDS spectrum displayed in Fig. 2, which shows that oxygen reacts with the carbon of the tungsten carbide and desorbs as CO at temperatures below 1300 K. The corresponding valence band spectrum (top of Fig. 3) points towards an oxide that is neither WO_3 nor WO_2 as judged from the strong intensity between the Fermi level and a binding energy of about 4 eV, which is not observed for these oxides [22,24]. Therefore, its composition must be WO_x with $x < 2$. The shift of the $W4f_{7/2}$ level points towards a composition similar to WO, which is known to form at the chosen oxidation conditions [19,22].

The $4f_{7/2}$ spectrum of the surface dosed at 1300 K displays two states that are about 0.7 eV apart from each other. This corresponds well to the energy separation of the $4f_{7/2}$ states of elemental tungsten and WO [22]. Thus, the state at 31.3 eV in this spectrum may be assigned to elemental tungsten. Its binding energy agrees well with the literature value of 31.4 eV [25], giving additional support to this assignment. Valence band spectra as displayed in Fig. 4 also indicate the existence of elemental tungsten. The strong feature in the spectrum of the W(110) surface at about 1.5 eV is also found in the spectra of oxygen-dosed WC(0001), whereas it is not found in the spectrum of the untreated tungsten carbide sample. From these results, one might expect that the adsorption properties of WC surfaces treated with oxygen at a high temperature should be considerably influenced by elemental tungsten. However, this is not the case. Fig. 5 shows photoelectron data for the adsorption of CO on clean and oxygen-treated WC(0001) [12]. Whereas there are strong signals of CO molecular levels in the spectrum of CO on clean WC(0001), no intensity of CO levels is found in the spectrum of CO on WC(0001) dosed with 2000 L of O_2 at $T \approx 1300$ K. Since elemental tungsten as well as WC(0001) adsorb CO at $T \approx 150$ K, this proves that the elemental tungsten is not accessible to the CO molecules; it must be situated below the surface.

The formation of elemental tungsten is not too

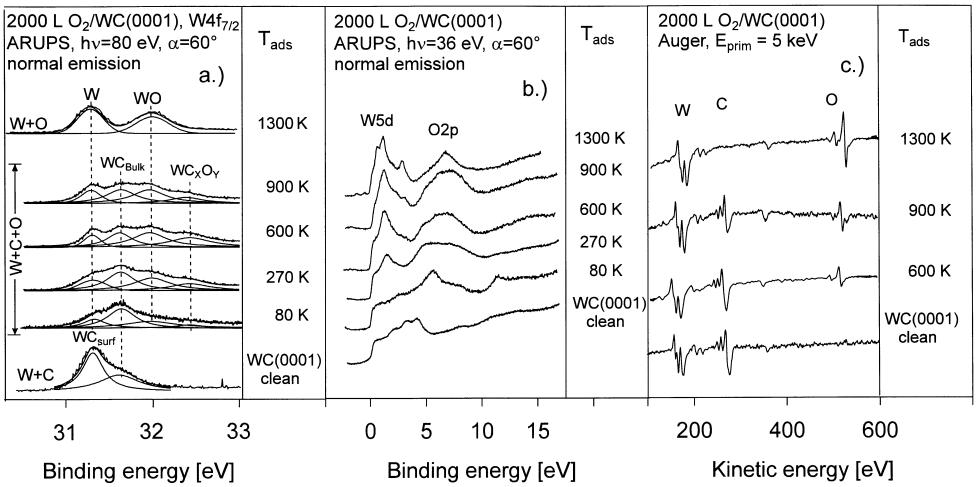

Fig. 3. Spectroscopic data of 2000 L of on WC(0001) as a function of the surface temperature during oxygen dosage. (a) High-resolution spectra of the $W4f_{7/2}$ level; (b) valence band ARUPS spectra; (c) AES data. In all cases, the oxygen pressure during dosage was 10^{-5} mbar.

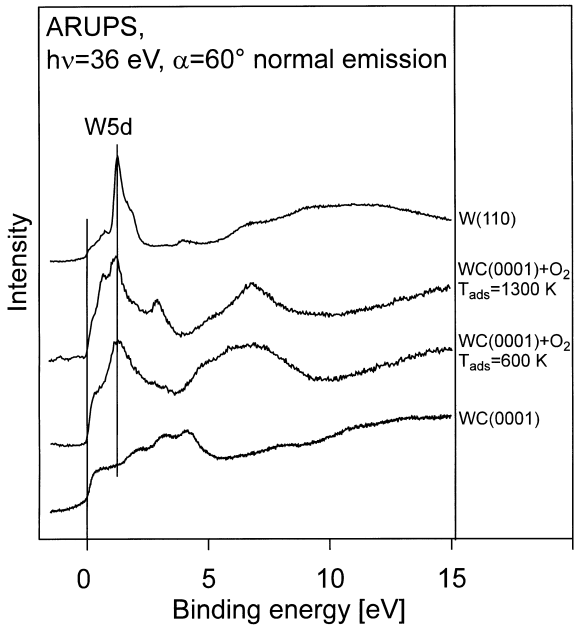

Fig. 4. Comparison of ARUPS spectra of the valence bands of W(110), WC(0001), and oxygen-dosed WC(0001). The spectra of the oxygen-dosed surfaces have been taken from Fig. 3b.

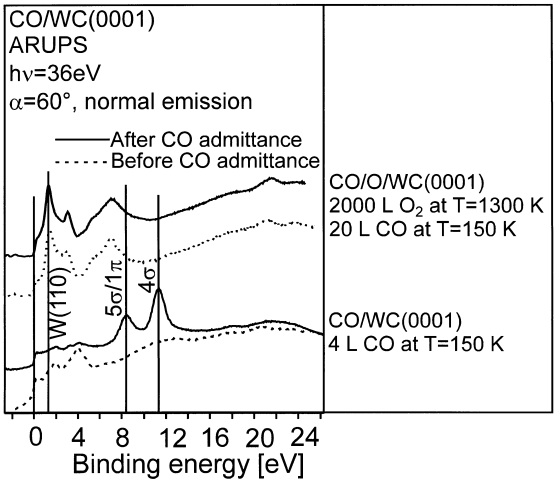

Fig. 5. Arups spectra of CO on oxygen-dosed and clean WC(0001). Oxygen has been admitted at a pressure of 10^{-5} mbar, whereas carbon monoxide was dosed at a pressure of 10^{-7} mbar. The position of the main peak of W(110) as taken from Fig. 4 is indicated in the figure.

surprising for the surface dosed at 1300 K since at this temperature, oxidized tungsten may be reduced by carbon, and tungsten carbide may be reduced by oxygen. Both reactions result in the formation of CO. This may lead to a situation as schematically drawn in Fig. 6 for an oxygen-treated tungsten carbide surface: Starting from the surface, the oxygen depletes the surface of carbon, leaving elemental tungsten behind. The reaction of oxygen with the elemental tungsten leads to the formation of a thin oxide film. Its limited thickness

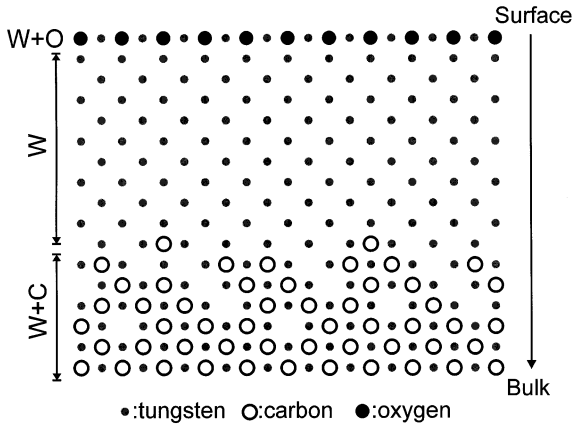

Fig. 6. Schematic drawing of the distribution of carbon and oxygen in the surface region of tungsten carbide after oxygen treatment at high temperature.

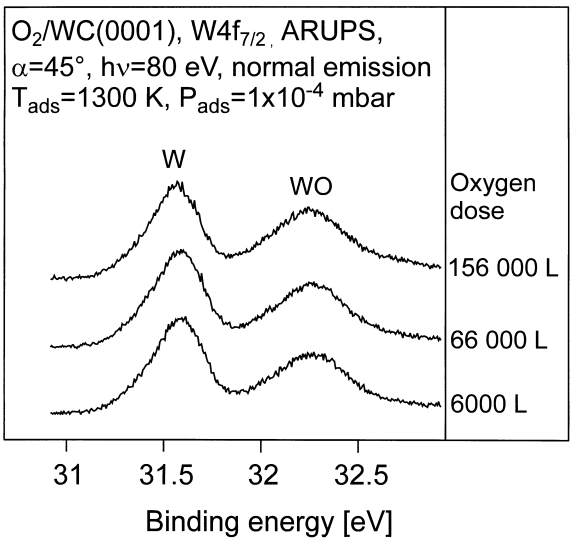

Fig. 7. Photoelectron spectra of the $W4f_{7/2}$ level obtained after treating the WC(0001) surface with different doses of oxygen at $T \approx 1300$ K.

gives rise to the relatively intense emission of the 4f levels of the elemental tungsten below the oxide as observed in Fig. 3. The thickness of the oxide film may be estimated from the ratio of the intensities of the 4f levels of the oxide and the metal (upper spectrum in Fig. 3a). With I_1 being the intensity of the oxide W 4f level, I_2 that of the elemental tungsten below the oxide and λ the electron mean free path length, the thickness Δ of the oxide film may be calculated according to $\Delta = \lambda \ln[(I_1/I_2)+1]$ [26]. Data for the electron mean free path length published in [27] give values between 0.8 and 4 layers for the electron mean free path length in different materials at $E_{kin} = 60$ eV. From this, it follows that the thickness of the oxide film should be between about 0.6 and 2.8 layers.

Under the chosen experimental conditions, the thickness of the oxide layer does not depend on the oxygen dose as indicated by the data shown in Fig. 7. This figure exhibits spectra of the $W4f_{7/2}$ level taken after treatment with different doses of oxygen at $T \approx 1300$ K. Obviously, the intensity of the oxide induced feature is not a function of the oxygen dose, which means that the thickness of the oxide film is always between 0.6 and 2.8 layers under the chosen experimental conditions. However, it should be clear that this is not valid if the oxygen dose is too small.

The formation of a thin oxide layer has also been observed for the oxidation of W(110) [28]. In that case, the thickness of the oxide layer was estimated to be only 1 ML. This fits well with the estimated thickness of the oxide layer on tungsten carbide.

However, the existence of elemental tungsten on the WC(0001) surface dosed at temperatures between 80 and 600 K may not be traced back to oxidation with CO formation since the first CO desorption peak is observed at $T \approx 750$ K (see Fig. 2). Surfaces dosed at these temperatures are composed of tungsten, carbon and oxygen as is obvious from the corresponding AES spectra in Fig. 3. Apart from the $4f_{7/2}$ states already identified in the spectra at the top and the bottom ($W_{surface}$, W_{bulk}, W and WO), an additional feature at a binding energy of 32.4 eV appears. In view of the chemical composition of the surfaces, we identify this feature as being due to an oxycarbide (WC_xO_y). The actual chemical composition of the oxycarbide is not evident from our data. As concluded from the binding energy of the $4f_{7/2}$ level, it is different from the oxycarbide observed by Katrib et al. [29]. Since the binding energy observed in the present case is lower, it is likely that the oxycarbide contains less oxygen than that reported in Ref. [29]. A possible reason for the

formation of elemental tungsten could be that the formation of the oxycarbide is accompanied by a consumption of carbon that might lead to the formation of elemental tungsten.

The $4f_{7/2}$ spectrum taken from the surface dosed at 900 K is similar to that taken after dosing at 600 K. This is somewhat unexpected since at temperatures between 600 and 900 K, CO formation starts, as revealed in Fig. 2. Therefore, one would expect that the spectrum taken after dosing the surface at 900 K should be similar to that of the surface dosed at 1300 K, which is not the case. A possible explanation might be that at $T \approx 900$ K, the speed of CO formation is not high enough to overcome the diffusion of carbon atoms into the surface region.

The $W4f_{7/2}$ binding energies as observed in Fig. 3a are compiled in Table 1. Håkanson and Johansson [19] observed oxygen-induced $4f_{7/2}$ states that were shifted by 0.29 eV and 0.66 eV relative to the position of WC bulk state. This agrees well with the states that we assigned to WO and WC_xO_y. From a comparison of their data with the data published by Himpsel et al. for the oxidation of tungsten [22], they concluded that these states should be due to chemisorbed oxygen (0.29 eV) and WO (0.66 eV). The origin of this misinterpretation is most likely that they did not take into account that the binding energies of the 4f bulk states of elemental tungsten and tungsten carbide are different. They assigned the state which we find at about 31.3 eV to the $4f_{7/2}$ surface state of tungsten carbide even for the oxidized tungsten carbide. Therefore, they did not recognize the formation of elemental tungsten on the surface.

Table 1
Binding energies of the $W4f_{7/2}$ levels as determined from Fig. 3a

$WC_{Surface}$	W	WC_{Bulk}	WO	WC_xO_y
31.31	31.32	31.64	31.98	32.38

The oxides WO_3 and WO_2 may only be obtained upon oxidation of the surface at higher pressures. We have applied pressures of about 100 mbar. Since it was not possible to anneal the crystal in an atmosphere of several millibars of O_2 without burning the filament used for heating, we have heated the sample to $T \approx 600$ K in UHV and admitted the oxygen after the heating has been switched off so that the oxidation occurred while the sample cooled down. The spectrum of the 4f levels (Fig. 8a, top) shows strongly shifted states that are characteristic of WO_3 [22,23]. In the corresponding AES spectrum (Fig. 8c, top) a strong oxygen signal shows up, and the ARUPS spectrum (Fig. 8b, top) is characteristic of a non-conducting material. Reduction with H_2 at $T \approx 500$ K leads to a less strongly oxidized surface.

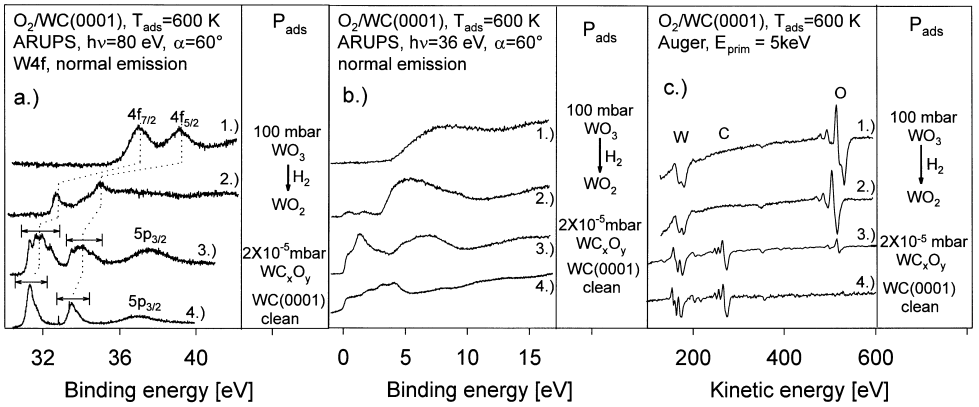

Fig. 8. Spectroscopic data of different preparations of WC(0001). (1) Sample heated up to $T = 600$ K in UHV and cooled down in an atmosphere of 100 mbar of O_2. (2) Oxidized surface after treatment with 3000 L of hydrogen ($P = 10^{-5}$ mbar, $t = 300$ s) at $T \approx 500$ K. (3) WC(0001) dosed with 2000 L of O_2 ($P = 2 \times 10^{-5}$ mbar, $t = 100$ s) at $T \approx 600$ K. (4) Stoichiometric WC(0001). (a) High-resolution spectra of the $W4f_{7/2}$ level. (b) Valence band ARUPS spectra. (c) AES data.

The W4f levels (Fig. 8a, second spectrum from the top) are shifted less as compared to those of WO_3, although some residual intensity due to WO_3 can still be observed. As indicated by the corresponding ARUPS spectrum, the oxide is similar to WO_2, which is electrically conducting and exhibits weak intensity near to the Fermi edge [22,23]. The observed shifts of the W4f states with respect to the energies of the WC bulk states are listed in Table 2. These values compare well to data given in Ref. [22] for the oxidation of elemental tungsten after consideration of the W–WC energy shift.

4. Summary

In this work, we report on the interaction of oxygen with WC(0001) under different preparation conditions. At low oxygen pressures of several 10^{-5} mbar, the surface oxidation was studied as a function of temperature. Between 80 and 900 K, we identify a mixture of tungsten oxide (WO), tungsten oxycarbide (WC_xO_y) and elemental tungsten. Oxidation at $T=1300$ K leads to a loss of all carbon in the surface region accessible with AES. At this temperature, the carbon reacts with oxygen and desorbs as CO leading to a thin layer of WO directly at the surface and elemental tungsten below. WO_3 forms at heavier oxidation conditions. We have applied 100 mbar of oxygen while the sample was cooling down after a flash to 600 K. The WO_3 could be transformed into WO_2 by reduction in a H_2 atmosphere with a pressure of about 10^{-5} mbar.

Table 2
Shifts of the W4f levels relative to the position of the bulk peak of clean WC(0001) for different tungsten oxides at the surface

Oxide	$W4f_{7/2}$ peak shift (eV)
WO	0.36
WO_2	1.16
WO_3	5.34

Acknowledgements

This work has been funded by the Bundesministerium für Forschung und Technologie under contract number 05 625 PCA 3. We acknowledge Dr Görting who supplied us with the tungsten carbide single crystal.

References

[1] S.T. Oyama, Catal. Today 15 (1992) 179.
[2] L.E. Toth, Transition Metal Carbides and Nitrides, Academic Press, New York, 1971.
[3] R.J. Colton, J.-T.J. Juang, J.W. Rabalais, Chem. Phys. Lett. 34 (1975) 337.
[4] R.L. Levy, M. Boudart, Science 181 (1973) 547.
[5] S.T. Oyama, The Chemistry of Transition Metal Carbides and Nitrides, Blackie, Glasgow, UK.
[6] L. Leclerq, M. Provost, G. Leclerq, J. Catal. 117 (1989) 384.
[7] H. Diets, L. Dittmar, D. Ohms, M. Radwan, K. Wiesener, J. Power Source. 40 (1992) 175.
[8] I. Nikolov, G. Papzov, V. Nadjenov, J. Power Source. 40 (1992) 333.
[9] J.G. Chen, Surf. Sci. Rep. 30 (1–3) (1997) 5–152.
[10] J.G. Chen, Chem. Rev. 96 (1996) 1477.
[11] L.I. Johansson, Surf. Sci. Rep. 21 (1995) 177.
[12] J. Brillo, R. Sur, H. Kuhlenbeck, H.-J. Freund, Surf. Sci. 397 (1998) 137–144.
[13] K.E. Curry, L.T. Thopmson, Catal. Today 21 (1994) 171.
[14] M. Muller, V. Keller, R. Ducros, G. Maire, Catal. Lett. 35 (1995) 65.
[15] V. Keller, M. Cleval, F. Maire, P. Wehrer, R. Ducros, G. Maire, Catal. Today 17 (1993) 493.
[16] F. Garin, V. Keller, R. Ducros, A. Muller, G. Maire, J. Catal. 166 (1997) 136.
[17] P.M. Stefan, M.L. Shek, I. Lindau, W.E. Spicer, L.I. Johansson, F. Hermann, R.V. Kasovski, G. Brogen, Phys. Rev. B 29 (1984) 5423.
[18] E.K. Curry, L. Thompson, Symposium on Chemistry and Characterization of Supported Metal Catalysts, 206th National Meeting of the American Chemical Society, 1993, p. 877.
[19] K.L. Hakanson, H.I.P. Johansson, L.I. Johansson, Phys. Rev. B 49 (1994) 2035.
[20] P.M. Stefan, PhD thesis, University of Stanford, Stanford, 1983.
[21] P. Feulner, D. Menzel, J. Vac. Sci. Technol. A 17 (1980) 662.
[22] F.J. Himpsel, J.F. Morar, F.R. McFeely, R.A. Pollak, G. Hollinger, Phys. Rev. B 30 (1984) 7236.
[23] C. Gu, C.G. Olson, D.W. Lynch, Phys. Rev. B 48 (1993) 12178.

[24] F.H. Jones, R.G. Egdell, A. Brown, F.R. Wondre, Surf. Sci. 374 (1997) 80.
[25] J.C. Fuggle, N. Mårtensson, J. Eletron Spectrosc. Relat. Phenom. 21 (1980) 275.
[26] A.B. Christie, in: J.M. Walls (Ed.), Methods of Surface Analysis, Cambridge University Press, Cambridge, 1989.
[27] G. Ertl, J. Küppers, Low Energy Electrons and Surface Chemistry, 2nd ed., VCH, Weinheim, 1985.
[28] D.M. Riffe, G.K. Wertheim, Surf. Sci. submitted.
[29] A. Katrib, F. Hemming, L. Hilaire, P. Wehrer, G. Maire, J. Electron Spectrosc. Relat. Phenom. 68 (1994) 595.